약학석사학위논문

리포좀 지질 구성에 따른 감광제의 Subcellular Localization과 High-Content Screening을 통한 그에 대한 광선역학요법유도 세포사 메카니즘

Control of Photosensitizer Subcellular Localization by Liposome Composition and the Monitoring of its Effects on Photodynamic Therapy Induced Cell Death Mechanisms via High-Content Screening

2016년 8월

서울대학교 대학원

약학과 약품분석학전공

남 지 우

리포좀 지질 구성에 따른 감광제의 Subcellular Localization과 High-Content Screening을 통한 그에 대한 광선역학요법유도 세포사 메카니즘

Control of Photosensitizer Subcellular Localization by Liposome Composition and the Monitoring of its Effects on Photodynamic Therapy Induced Cell Death Mechanisms via High-Content Screening

지도교수 송 준 명

이 논문을 약학석사학위논문으로 제출함

2016년 8월

서울대학교 대학원

약학과 약품분석학전공

남 지 우

남지우의 약학석사학위논문을 인준함

2016년 8월

위 원 장 박 정 일 (인)

부 위 원 장 권 성 원 (인)

위 원 송 준 명 (인)

Abstract

5,10,15,20-tetrakis(benzo[b]thiophene) (BTP) is a newly synthesized hydrophobic photosensitizer with significant quantum yield. Previously, its limitations in solubility had hindered scientific experimentation regarding its photodynamic effects on cancer cells. By utilizing various compositions of liposomes in order to alter the solubility of BTP, the photocytotoxicity, reactive oxygen species generation, and subcellular localization of the liposomal BTP were identified in this work. DNA fragmentation and high content screening assays were performed in order to shed light on the tumoricidal mechanism of the liposomal photosensitizer. The MTT assay results showed promising results in the irradiation specific PDT activity against MCF-7 cells in all liposomal compositions. Production of ROS was confirmed in the liposomal BTP treated MCF-7 cells after irradiation in a concentration dependent manner. The subcellular localization assays revealed that the localization of BTP was dependent on both the photosensitizer's chemical properties and the properties of the delivery agent encapsulating aforesaid substance. Significant DNA fragmentation was observed in both DOPC-BTP and DOPE-BTP, DNA localizing liposomal BTP, treated MCF-7 cells. All liposomal-BTPs were successful in inducing MPT and activating caspase-3/7. ER localizing BTP were able to significantly increase the cytosolic calcium levels by photodynamic therapy, confirming the photodynamic ability of ER localized BTP to damage the ER membrane. The application of liposomes in delivering a novel hydrophobic photosensitizer, BTP, and photodynamic therapy treatment against MCF-7 cells were successful. From these results, it was confirmed that the MCF-7 cell death pathway via photodynamic therapy was altered in a controlled manner by controlling the intracellular localization of

the photosensitizer through lipid composition adjustment.

Keyword

Photodynamic therapy; Liposome; MCF-7; Subcellular localization; High content screening; Cell death pathway.

Student Number: 2014-21971

Table of Contents

List of Figures

List of Abbreviations

BTP: 5,10,15,20-tetrakis(benzo[b]thiophene) porphyrin
DOPC:1,2-dioleoyl-sn-glycero-3-phosphocholine
DOPE: 1,2-dioleoyl-sn-glycero-3-phosphoethanolamine
DPPC: 1,2-dipalmitoyl-sn-glycero-3-phosphocholine
PS: phosphatidylserine
PI: phosphatidylinositol
TPPS: 4,4',4'',4'''-(Porphine-5,10,15,20-tetrayl)tetrakis(benzenesulfonic acid)
HCS: High Content Screening
PDT: Photodynamic Therapy
ROS: Reactive Oxygen Species
SOD: Superoxide Dismutase
ER: Endoplasmic Reticulum
MPT: Mitochondrial Permeability Transition

Ⅰ. Introduction

Photodynamic therapy (PDT) has been receiving attention as a target selective tumoricidal method with significant efficacy. There is a plethora of scientific reports regarding PDT and its effectiveness in inhibiting tumor growth by generating intracellular reactive oxygen species (ROS). Ahmad et al. reported that PDT treatments caused significant growth arrest observed specifically during the G0-G1 phase, inhibiting carcinogenic mitosis at stages prior to DNA replication[1]. The target specific photodynamic treatment is controlled by its irradiation method. By applying the appropriate light to the area of the tumor utilizing PDT, the cancer treatment becomes much more selective, thus substantially decreasing the amount of damage done to normal cells. The main components of PDT are the photosensitizer and irradiation. Photosensitizers can be excited from its ground state to a triplet excited state by a momentary excited singlet state. The formed triplet state is able to either go through electron or hydrogen atom transfer reactions with oxygen or a substrate to produce free radicals and ROSs or transfer its energy directly to ground-state triplet oxygen to form excited state singlet oxygen[2,3]. The direction in which the triplet state reacts is dependent upon the oxygen supply of its environment. Increase in the formation of intracellular reactive oxygen species triggers cellular antioxidant defense mechanisms. For example, superoxide dismutase (SOD) is an antioxidant enzyme capable of catalyzing the conversion of two superoxide anions into hydrogen peroxide, which can then be converted into water and oxygen by catalase[4]. Manganese superoxide dismutase is reported to be present in mammalian mitochondria, an innate producer of intracellular ROS via its aerobic respiratory chain[5]. A balance between the production and removal ROS is vital to the maintenance of many cellular processes. The disruption of this balance leads to oxidative stress, a major contributor in cell death. PDT is able to induce three types of cell

death (apoptosis, necrosis, and autophagy) depending on its parameters. The apoptotic cell death by PDT has been reported to involve factors such as executioner caspases, Bcl-2, Bax, tumor necrosis factor receptor (TNFR), nuclear factor kappa B (NF-κB), Mitogen-activated protein kinases (MAPK), extracellular signal-regulated kinases (ERK), c-Jun N-terminal kinases (JNK), and stress-activated protein kinases (SAPK) 3[6,7]. The intracellular localization of the photosensitizer dictates the cell death pathway of PDT, due to the transient nature of reactive oxygen species. The half-life of most reactive oxygen species are 1-4 μs with migration capacities less than 30 nm[8]. PDT damage in the mitochondria is known to trigger the release of cytochrome c, a component of the electron transport chain and initiator of apoptosis via the caspase pathway, and Bcl-2 damage. Oxidative damage by means of PDT to the Bcl-2 family is known to disable Bcl-2 and related anti-apoptotic proteins and activate the pro-apoptotic proteins[9]. 5,10,15,20-tetrakis(7-sulfonatobenzo[b]thiophene) porphyrin is a reported photosensitizer with significant anticancer photodynamic activity[10]. 5,10,15,20-tetrakis(7-sulfonatobenzo[b]thiophene) porphyrin was reported to be localizing mainly in the mitochondria and partially in the nucleus of MCF-7 cells. This molecule is the hydrophilic derivative of 5,10,15,20-tetrakis(benzo[b]thiophene) porphyrin. 5,10,15,20-tetrakis(benzo[b]thiophene) porphyrin is insoluble in most organic solvents and water, which makes it an unideal PDT agent. Thus, the sulfonation of 5,10,15,20-tetrakis(benzo[b]thiophene) was utilized as a means of increasing its solubility in water and the more polar organic solvents. The sulfonation of 5,10,15,20-tetrakis(benzo[b]thiophene) is rather tedious and produces markedly low yields mainly due to the extra purification steps. In this study, liposomes were used to encapsulate the highly hydrophobic porphyrin in order to alternatively deliver the photosensitizer to breast cancer cells for irradiation specific photodynamic therapy against breast cancer cells.

Liposomes have been widely utilized as a drug delivery agent of both hydrophobic and hydrophilic materials. Biocompatibility, biodegradability, and ease of handling make liposome an ideal drug delivery moiety. Liposomes are often formed with lipids readily present in the human body, which can be responsible for its advantageous biocompatibility. The dissolution of hydrophobic drugs for their application often incorporate toxic co-solvents, which may lead to an undesirable increase in drug toxicity[11]. 1,2-dioleoyl-sn-glycero-3-phosphocholine (DOPC), 1,2-dioleoyl-sn-glycero-3-phosphoethanolamine (DOPE), 1,2-dipalmitoyl-sn-glycero-3-phosphocholine (DPPC), phosphotidylserine (PS), and phosphatidylinositol (PI) were utilized as liposomal drug delivery systems in this study. The listed liposomes have been widely studied for their efficiency in liposomal formation and drug delivery[12,13]. Phosphocholines, zwitterionic precursors of phosphatidylcholine, are universal in phospholipids of the cellular membranes and plasma lipoproteins of plants, animals, and fungi[14]. There have been no previous reports regarding the subcellular organelle specific localization of any of the single lipid liposomes used in this study. Pollock et al. studied the effect of the lipid composition of the liposomes on the subcellular liposomal uptake by the endoplasmic reticulum (ER)[15]. The results from the study demonstrated that the liposome with a certain lipid composition (DOPC:DOPE:PS:PI = 1.5:1.5:1:1) demonstrated 88±3.5 % colocalization with ER membranes. Furthermore, the ER liposomes were reported to utilize scavenger and low-density lipoprotein receptors to enter the cells through microtubule and caveolin dependent mechanisms such as endocytosis and membrane fusion. The endoplasmic reticulum manufactures, processes, and transports a variety of biochemical substances. The rough ER contains ribosomes are involved in protein synthesis and the smooth ER is responsible for lipid manufacturing and metabolism. Responsible for such crucial biochemical processes, the ER presented itself as a suitable target for

PDT. The question was whether the photosensitizers would be localized in the ER, the liposomes' localization destination, or elsewhere in the cell dictated by the chemical properties of the photosensitizer itself. Due to BTP's limitations in solubility, its standalone biological properties against MCF-7 cells were previously indeterminable. Phosphatidylserine, phosphatidylinositol, Phosphocholines and phosphoethanolamine, lipids present in cellular membranes, were applied to alter the solubility of BTP to study its biological properties against MCF-7 cells.

The PDT effects of the liposomal-BTP on MCF-7 breast cancer cells were studied by photo-cytotoxicity tests, subcellular localization assays, ROS detection, DNA fragmentation assays, and high content screening (HCS). HCS is capable of simultaneously monitoring the activation/inhibition of intracellular biomarkers induced by drugs based on multicolor detection. Different cell death mechanisms caused by the liposome-driven subcellular localization were compared by simultaneously monitoring the various responses of biomarkers under PDT treatment. By attempting to control the subcellular localization of the liposomal-BTPs through altering the liposomal composition and studying its effect on the cell death pathway, the correlation between the subcellular localization of the photosensitizer and the cell death mechanism via PDT was investigated in this research.

Ⅱ. Experimental

1. Synthesis of 5,10,15,20-tetrakis-(benzo[b]thiophene) porphyrin

Benzo[b]thiophene porphyrin was synthesized using a one-pot condensation procedure derived from the Lindsey's method[9]. 1 g (6.2 mmol) of Benzo-[b]-thiophene-2-carboxaldehyde was dissolved in 620 mL of anhydrous dichloromethane. 0.43 mL (6.2 mmol) of pyrrole was added to the solution and was allowed to stir in a nitrogen purged container for 30 minutes. Then boron trifluoride diethyl etherate (BF3·OEt2) was added to the mixture solution as an acid catalyst. In the dark, the reaction mixture was stirred for two hours at room temperature. Terachloro-1,4-benzoquinone was then added and the reaction mixture was refluxed for four hours at 37.5 C. The crude product was obtained by removing the solvent by rotovap and purified through column chromatography using a n-hexane/DCM mixture. The purity and the formation of the product were confirmed via UV-vis spectrometry (Thermo Fisher Scientific, USA), elemental analysis, 1H NMR (FT-NMR Avance 400, Bruker, USA), MALDI-TOF mass spectrometry (MALDI TOF/TOF 5800 system, AB Sciex, USA), and fast bombardment high resolution mass spectrometry (JMS-600W, JEOL, Japan).

2. Liposome Formation

All lipids used in the liposome formation were purchased from Avanti Polar lipids, USA. Four different compositions of liposomes were studied for their ability to deliver the hydrophobic BTP molecules to MCF-7 breast cancer cells. Two of the liposomes were uniform DOPC and DOPE (Avanti Polar Lipids, USA) liposomes, where only one type of lipid was used to encapsulate the hydrophobic photosensitizer. ER liposomes (M1) were one of the lipid mixture composition utilized as a delivery system. The lipid composition of the M1 liposomes were prepared with the following molar ratio: DOPE:DOPC:PS:PI = 1.5:1.5:1:1 (Avanti Polar Lipids, USA). The M2 liposomes were prepared with the following molar ratio of lipids: DOPC:DPPC:PS:PI = 2.5:0.5:1:1 (Avanti Polar Lipids, USA). The lipid mixtures were prepared to yield a final total concentration of 10 mg/ml in CHCl3. All mixtures included 1 mg/ml of cholesterol for improved liposomal stability[10-12]. 5 mg (5.956 μmol) of BTP were dissolved into each of the lipid solutions and sonicated for 30 minutes to ensure the homogeneity of the solutions. The rest of the liposome preparation followed a modified thin lipid film hydration method. The solvent of the mixtures was slowly removed using a rotary evaporator until the layers were completely dry. Then the lipid

layer was allowed to incubate in PBS for 1 hour. The PBS dispersion of the liposomes were then swirled and subjected to short periods of sonication for several hours. Unilamellar vesicles were prepared by liposomal extrusion using 0.2 μm polycarbonate membranes (Avanti polar lipids, USA). The BTP encapsulated liposomes were prepared shortly before experimentations and kept at 4 C. The formed liposomes were characterized by dynamic light scattering and electrophoretic light scattering.

3. Photocytotoxicity Test

About 1.4 X 104 MCF-7 cells were seeded in 96-well plate and incubated at 37 C in 5% CO2 for 24 hours. Cells were treated with BTP at concentrations ranging from 0 to 16 μM for 24 hours. After the 24-hour treatment with the novel photosensitizer, the cells were irradiated using a 600 nm diode laser at 50 mW for 30 minutes. The cells were then incubated in the same conditions as before for 24 hours. After the recovery period, the cells were then treated with a 1.2 mM (final concentration) Thiazoyl blue tetrazolium bromide (MTT) solution and incubated for 3 hours. The MTT solution was then removed from the wells, and the formed formazan crystals were dissolved in DMSO. The relative cell viability was determined by measuring the absorbance of the formazan/DMSO

solution in each well at 570 nm with a multiplate reader (Gemini XS, Molecular devices, USA).

4. Intracellular Reactive Oxygen Species Detection

About 4×10^5 MCF-7 cells were seeded in a 12-well plate and incubated at 37 C in 5% CO2 for 24 hours. The cells were then incubated in solutions of various liposomal-BTP at different concentrations for 4 hours. After the incubation period, the cells were irradiated with a 600 nm diode laser at 50 mW for 30 minutes. Then the MCF-7 cells were washed and incubated in a 4% formaldehyde solution for 15 minutes with minimal exposure to light. The fixated cells were washed with PBS and treated with a 20 μM 2',7'-dichlorofluorescin diacetate (DCFDA) solution for 15 minutes at room temperature. After the treatment of DCFDA, the cells were thoroughly washed with PBS to remove any extracellular 2'7'-dichlorofluorescin generated by exogenous factors. Finally, the cells were then observed and imaged using a fluorescence microscope (IX73, Olympus, Japan). The excitation and emission wavelengths were 495 and 529 nm, respectively.

5. Subcellular Localization

Approximately 1×10^6 MCF-7 cells were seeded on to a coverslip in a 6-well plate and incubated for 24 hours at 37 C in 5% CO2. The cells were then treated with various liposomal-BTP with a final BTP concentration of ~10 μM for 4 hours. After the treatment of the liposomal photosensitizer, the treatment solution was removed and the cells were washed with PBS. The cells were then fixed using a 4% formaldehyde solution for 15 minutes at room temperature. The fixated cells were then washed with PBS and incubated in a 0.2% saponin solution for 10 minutes to increase the permeability of the cells to ensure the intracellular staining of the organelles[13]. The cells were once again washed with PBS and stained with its designated organelle specific probes (Hoechst λex 350/λem 461, ER-tracker 504/511, BTP 432/660). After the staining process, the cells were washed with PBS and the coverslip was mounted on to a glass slide using a Dako fluorescent mounting medium (Dako North America, USA). The mounted coverslip was observed and imaged using a confocal microscope (TCS SP8, Leica, Germany) equipped with an acousto-optic tunable filter.

6. DNA Fragmentation

MCF-7 cells were treated with different compositions of liposomal-BTP. After 24 h incubation, the cells were irradiated at 50 mW for 30 minutes. Immediately after irradiation, the cells were incubated at 37 C for 24 h. The irradiated and non-irradiated cells were collected and DNA was isolated from 3×10^6 cells using a QIAamp DNA mini kit (Qiagen, USA). The samples of extracted DNA were separated using a 1.2 % agarose gel to identify the DNA fragmentation using the manufacturer's protocol. 30 ng of DNA was loaded onto the gel containing 1X GelRed Nucleic acid staining dye. Electrophoresis was performed in 1X Tris-borate-EDTA (TBE) electrophoresis buffer. The bands were visualized under UV trans illuminator and image was acquired using LAS 4000 (GE Healthcare, USA). The gel electrophoresis image was analyzed by Image J.

7. High Content Screening

MCF-7 cells were seeded in a 12 well plate. The cultured MCF-7 cells were treated with liposomal-BTP at [BTP] 5, 10, and 20 μM for 24 hours. The cells were then subjected to 30 minutes of irradiation at 50 mW. The PDT treated cells were then thoroughly washed with PBS and immediately treated with a calcium indicator orange solution (Invitrogen, USA) and incubated for 45 minutes in the dark at room temperature. The cells were washed with PBS and treated with

calceinacetoxymethyl ester (calcein-AM) from the MitoProbe Transition Pore Assay kit (Invitrogen, USA). Then the cells were treated with a Magic Red™ caspase-3/7 substrate solution (ImmunoChemistry Technologies, USA) and incubated in the dark for 6 minutes at room temperature. CoCl2 was added to the cells for 10 minutes before the cells were finally washed with PBS. An acousto-optic tunable filter (TEAF10-0.45-0.7-s, Brimrose Corporation, USA) was utilized to obtain fluorescence images of the stained MCF-7 cells.

Ⅲ. Results

1. BTP Synthesis and Characterization

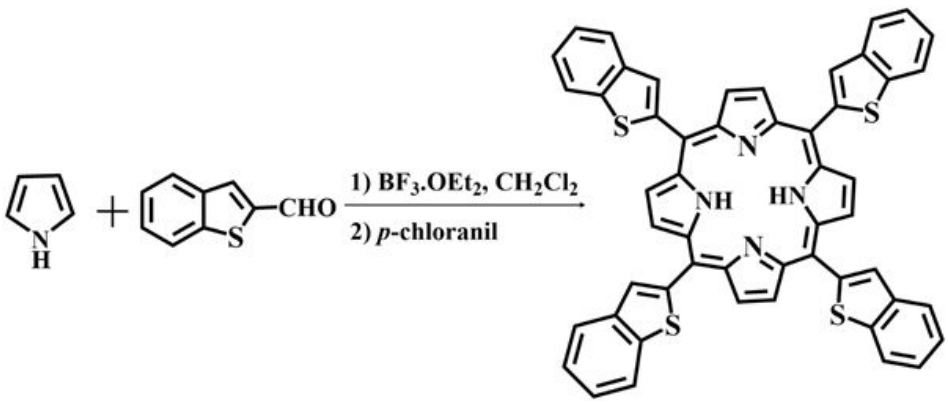

Figure 1. The reaction scheme of the synthetis for 5,10,15,20-tetrakis-(benzo[b]thiophene)porphyrin

Figure 1 represents the chemical reaction yielding the subject photosensitizer, BTP. The purified product yielded a deep wine colored fine powder. The percent yield of the product was ~15%. The calculated elemental composition for C52H30N4S4: C, 74.43; H, 3.60; N, 6.68; S, 15.29. Observed elemental composition: C, 74.02; H, 3.10; N, 6.38; S, 15.13. The optical properties of the purified BTP were measured using an ultraviolet-visible spectrometer. Figure 2 shows the UV-vis spectrum of BTP, similar to that of its sulfonated derivative. The spectrum exhibited a soret band at 432 nm and Q bands at 525, 561, and 600 nm, representing the characteristic

absorption peaks of porphyrins.

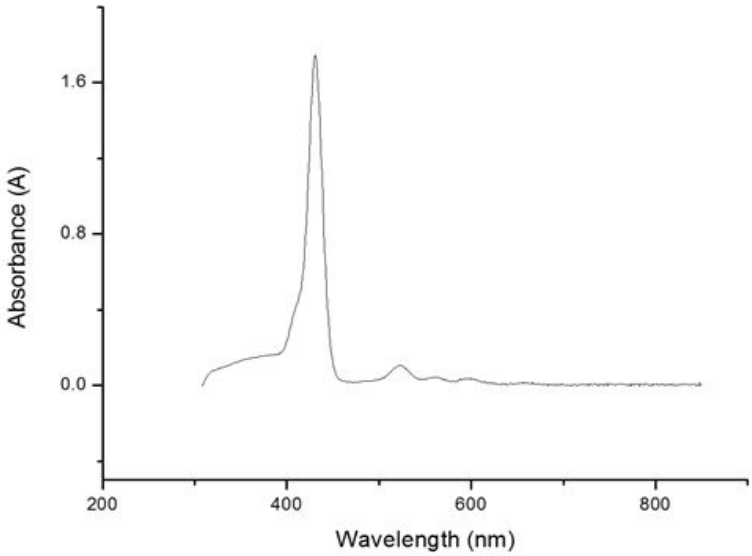

Figure 2. Ultraviolet-Visible Spectrometry

The UV-Vis spectrum of the purified 5,10,15,20-tetrakis-(benzo[b]thiophene)porphyrin.

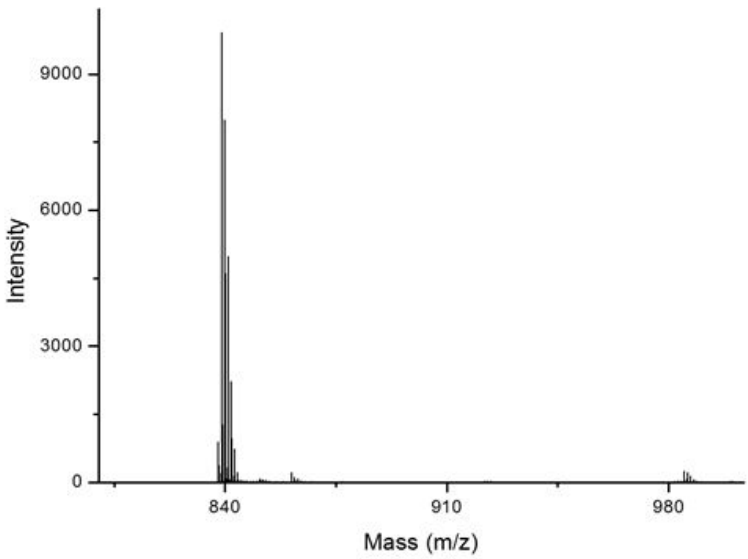

Figure 3. Mass Spectrometry

The mass spectrometry spectrum of 5,10,15,20-tetrakis-(benzo[b]thiophene)porphyrin. The purified substance was analyzed by a MALDI-TOF mass spectrometer at the national center for inter-university research facility in Seoul National University.

Figure 3 is the MALDI-TOF MS spectrum of BTP. The major peak at 839 represents the molecular weight of BTP, which has an exact mass of 839.08. The MALDI-TOF MS data confirms the successful formation of the desired photosensitizer with high purity. MALDI-TOF MS: m/z 839.2 [M]+. HR-MS(FAB) m/z: 839.1437. The FAB HR-MS results demonstrated an error of +1.4 ppm.

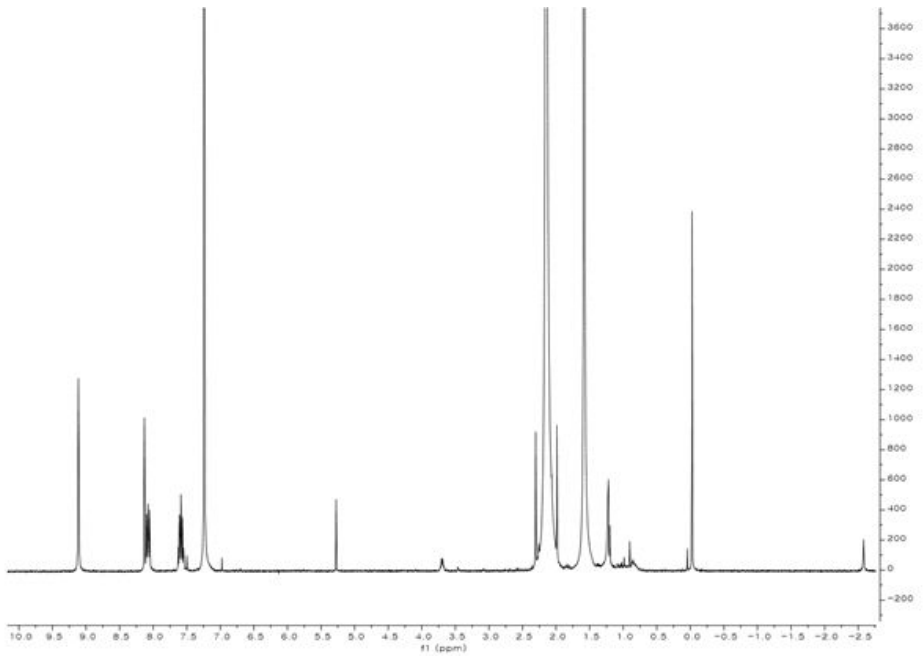

Figure 4. NMR Spectrometry

The nuclear magnetic resonance spectrum of 5,10,15,20-tetrakis-(benzo[b]thiophene)porphyrin. The purified substance was analyzed by a 400 MHz nuclear magnetic resonance spectrometer at the college of pharmacy in Seoul National University.

The NMR spectrum shown in figure 4 further confirms the molecular structure and purity of the synthesized BTP. H NMR (400 MHz, chloroform-d): δ 9.12 (s, 8H), 8.14 (s, 4H), 8.14–8.04 (m, 8H), 7.67–7.54 (m, 8H), −2.59 (s, 2H). 13C NMR (500 MHz, DMSO-d6): δ 110.41, 112.56, 121.06, 124.08, 125.20, 131.10, 134.84, 155.03, 160.72, 186.39, 190.74, 165.61.

2. Dynamic Light Scattering and Electrophoretic Light Scattering

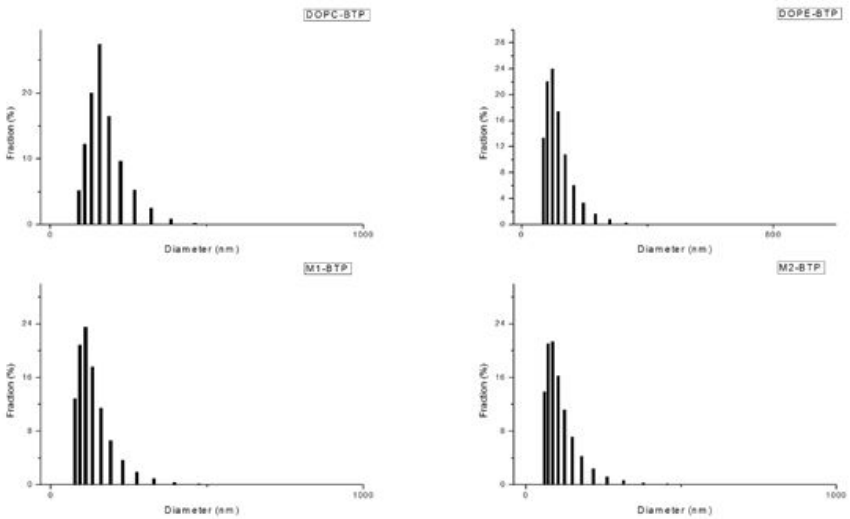

Figure 5. Dynamic Light Scattering

The particle size distribution of liposomal 5,10,15,20-tetrakis-(benzo[b]thiophene)porphyrin analyzed by a dynamic light scattering spectrophotometer

The particle size distributions of the various liposomal-BTP were measured by a dynamic light scattering spectrophotometer (DLS-7000, Otsuka Electronics, Japan) as shown in figure 5. The average diameters of the empty liposomes made of DOPC, DOPE, M1, and M2 were 149.6, 176.9, 176.3, and 184.8 nm, respectively. The average diameters of DOPC-BTP, DOPE-BTP, M1-BTP, and M2-BTP were 151.3, 177.7, 180, and 187.2 nm, respectively. The polydispersity indices of the empty DOPC, DOPE, M1, and M2 liposomes were 0.166, 0.182, 0.203 and 0.272, respectively. The polydispersity indices of the BTP encapsulated liposomes were 0.171, 0.18, 0.188, and

0.278, respectively.

	DOPE	DOPC	M1	M2
Empty	-30.92	-56.58	-46.35	-33.86
BTP	-30.7	-57.12	-45.51	-33.45

Figure 6. Electrophoretic Light Scattering

The zeta potentials of the various 5,10,15,20-tetrakis-(benzo[b]thiophene)porphyrin encapsulated liposomes analyzed by electrophoretic light scattering spectrophotometry.

3. Photocytotoxicity

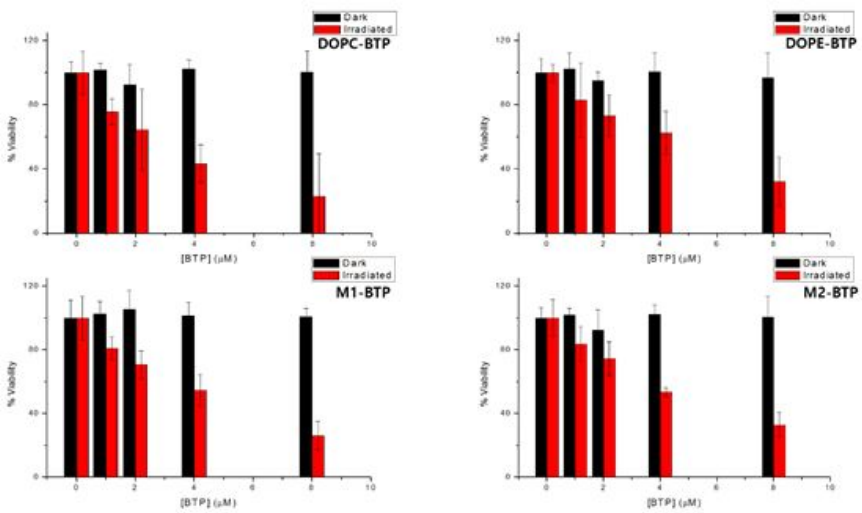

Figure 7. MTT Assay

The % viability of the liposomal-BTP treated MCF-7 cells. The % relative viability was calculated from the optical absorption at 570 nm in comparison to that of the controls. The dark controls represent the cells that were not irradiated with NIR, whereas the experimental groups were irradiated using a 600

nm diode laser at 50 mW for 30 minutes. The error bars represent the standard deviation from 6 separate experiments.

The MTT assays clearly confirm that the photodynamic therapy only affected the irradiated cells as shown in figure 7. The dark control MCF-7 cells, which were not irradiated, were healthy and unaffected by the photosensitizer. The calculated IC50 values of DOPC, DOPE, M1, and M2 liposomes were 8.09, 9.96, 9.56, and 9.34 μM, respectively. The MTT assays demonstrated the successful liposomal delivery of the newly synthesized photosensitizer and its potential as a target-specific system for photodynamic therapy against

3. Intracellular Reactive Oxygen Species Detection

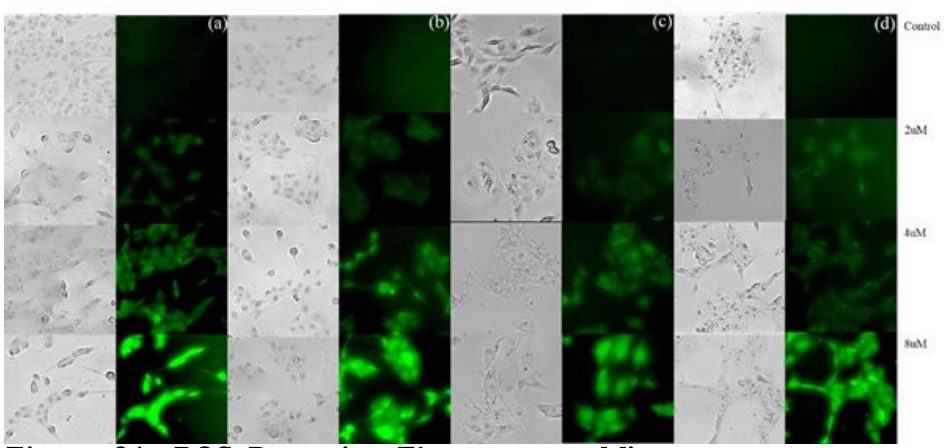

Figure 8A. ROS Detection Fluorescence Microscopy

The reactive oxygen species detection fluorescence

microscopic imaging. DCFDA was used to detect the photodynamic generation of reactive oxygen species from the liposomal-BTP treated MCF-7 cells. (a) BTP encapsulated DOPC liposome, (b) BTP encapsulated DOPE liposome, (c) BTP encapsulated ER-liposome (M1), (d) BTP encapsulated M2 liposome.

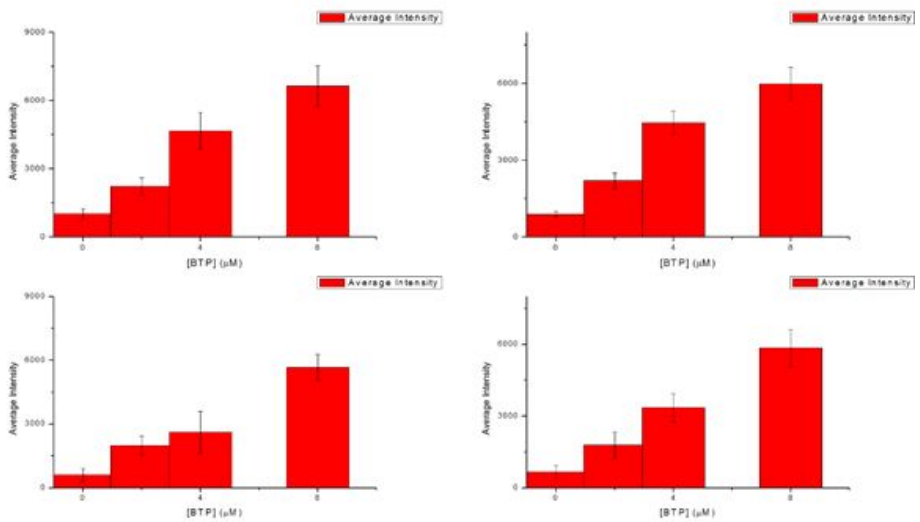

Figure 8B. Detected ROS levels

The calculated average fluorescence using the imaging software MetavueTM. (a) BTP encapsulated DOPC liposome, (b) BTP encapsulated DOPE liposome, (c) BTP encapsulated ER-liposome (M1), (d) BTP encapsulated M2 liposome.

The bright field images and their corresponding fluorescence images of the various liposomal-BTP in figure 8A confirm the successful delivery of BTP and production of ROS via

irradiation in a BTP concentration-dependent manner. The fluorescence intensity of the imaged cells are expected to be proportional to the concentration of DCF, which in turn is proportional to the concentration of ROS[16]. The average intensity of each group was calculated and plotted against its liposomal-BTP treatment concentration (figure 8B). In agreement with the cytotoxicity test results, MCF-7 cells treated with DOPC-BTP contained the highest concentrations of ROS, possibly to the point of saturation at certain points of the cells. All MCF-7 cells treated with liposomal-BTP exhibited high levels of ROS, relative to the control.

4. Subcellular Localization

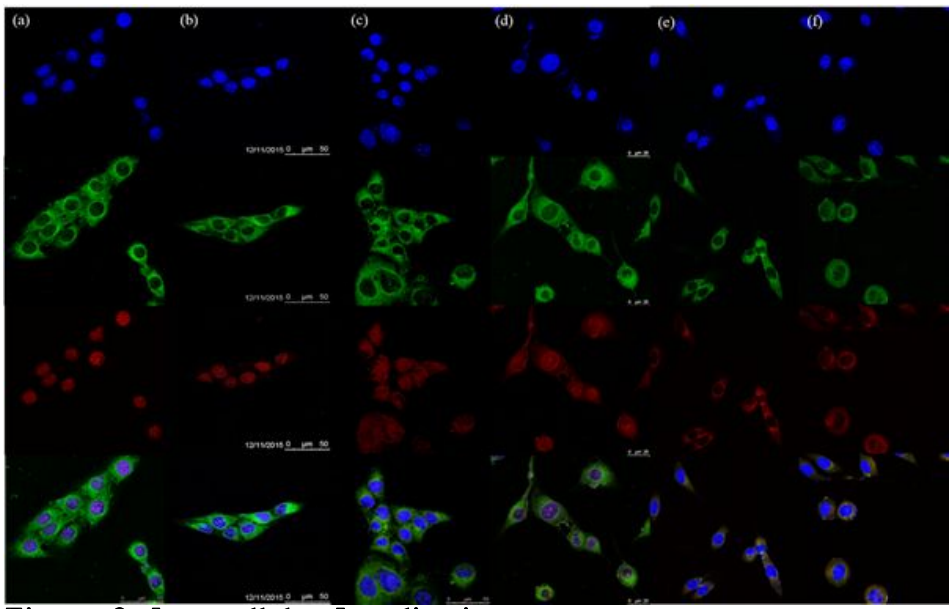

Figure 9. Intracellular Localization

The localization assay fluorescence microscopy images of (a) DOPC-BTP (b) DOPE-BTP (c) M1-BTP (d) M2-BTP (e) DOPC-TPPS (f) DOPE-TPPS treated MCF-7 cells. Images sets (a), (b), (c), (d) correspond to the Hoechst (blue), ER-tracker (green), BTP (red), and overlay, respectively from top to bottom. Images sets (e), (f) correspond to the Hoechst (blue), Lyso-tracker (green), BTP (red), and overlay, respectively from top to bottom. The corresponding excitation and emission wavelengths were Hoechst λex 350/λem 461, ER-tracker 504/511, Lyso-tracker 504/511 and BTP 432/660, respectively.

Figure 9 demonstrates the subcellular localization assay results. BTP delivered by single-lipid liposomes, DOPE and DOPC, were found to be localized in the nucleus. The chromatic alteration seen in the overlay images clearly confirm the BTP localization in the nucleus. BTP delivered by M1 (ER) and M2 liposomes were shown to be localized in both the ER and the nucleus. The overlay image exhibits a color change in both the nucleus and the ER as the BTP fluorescence coincides with the Hoechst and ER-tracker fluorescence. The fluorescence intensity of BTP in the nucleus of the M1-BTP group was much lower than that of the M2-BTP group. These results clearly confirm the presence of BTP in the cells and the subcellular localization of BTP. However, it is difficult to conclude whether the nuclear localization of BTP is an effect of the lipid properties of the liposomes or chemical properties of BTP from the DOPC-BTP and DOPE-BTP localization assay results (figure 9 (a) and (b)). In order to verify the effects of DOPE and DOPC on the subcellular localization of the liposome encapsulated BTP, the intracellular localization of 4,4',4'',4'''-(Porphine-5,10,15,20-tetrayl)tetrakis(benzenesulfonic acid) (TPPS), DOPE-TPPS, and DOPC-TPPS was monitored. TPPS has been reported to localize in the lysosome of cells[5],[17]. As the DOPC and DOPE encapsulated TPPS was observed to be localized in the lysosome, as shown in figure 9(e) and 9(f), it can be inferred that both DOPC and DOPE liposomes do not affect the intracellular localization of the entrapped photosensitizer.

5. DNA Fragmentation

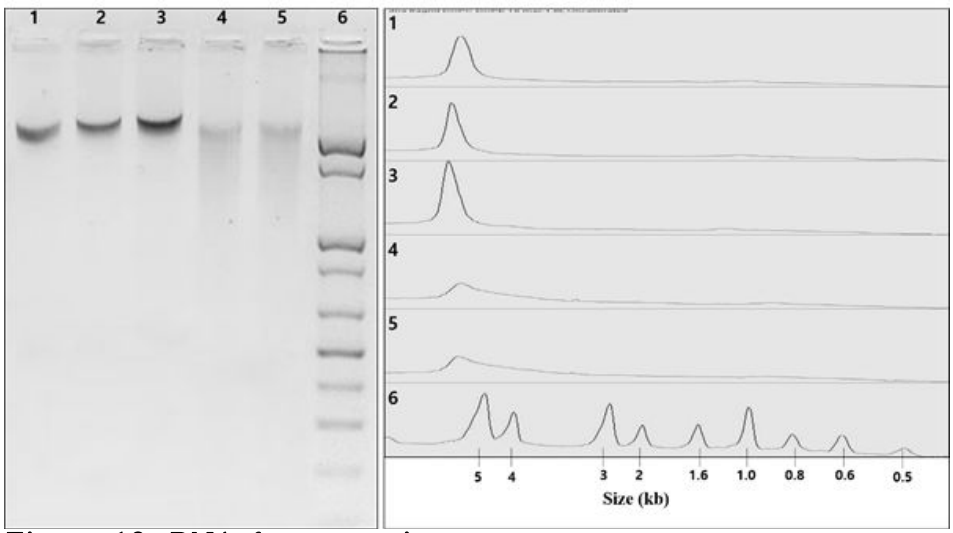

Figure 10. DNA fragmentation

Agarose gel electrophoresis of MCF-7 cells treated with or without liposomal-BTP was done to generate DNA fragmentation. Lane 1: Irradiation alone, Lane 2: M1-BTP (Irradiated), Lane 3: M2-BTP (Irradiated), Lane 4: DOPC-BTP (Irradiated), Lane 5: DOPE-BTP (Irradiated), Lane 6: 1 Kb DNA ladder

The confirmation of the liposomal-BTP's photocytotoxicity and its localization in the nucleus led to the possibility of cell death initiation via PDT-induced DNA damage. As shown in figure 10, the fragmentation of DNA was observed to be profound in cells treated with DOPC-BTP and DOPE-BTP (Nucleus-localizing liposomal-BTPs), as expected. On the contrary, cells exposed to the irradiation alone did not cause any observable fragmentation of the DNA. The lack of either

the photosensitizer or irradiation failed to cause any DNA fragmentation in the MCF-7 cells, which denotes the capacity for control of selectivity in PDT. The DNA fragmentation assays demonstrated the effectiveness of PDT in causing DNA fragmentation when utilizing a nucleus-localizing liposomal-BTP.

6. High Content Screening

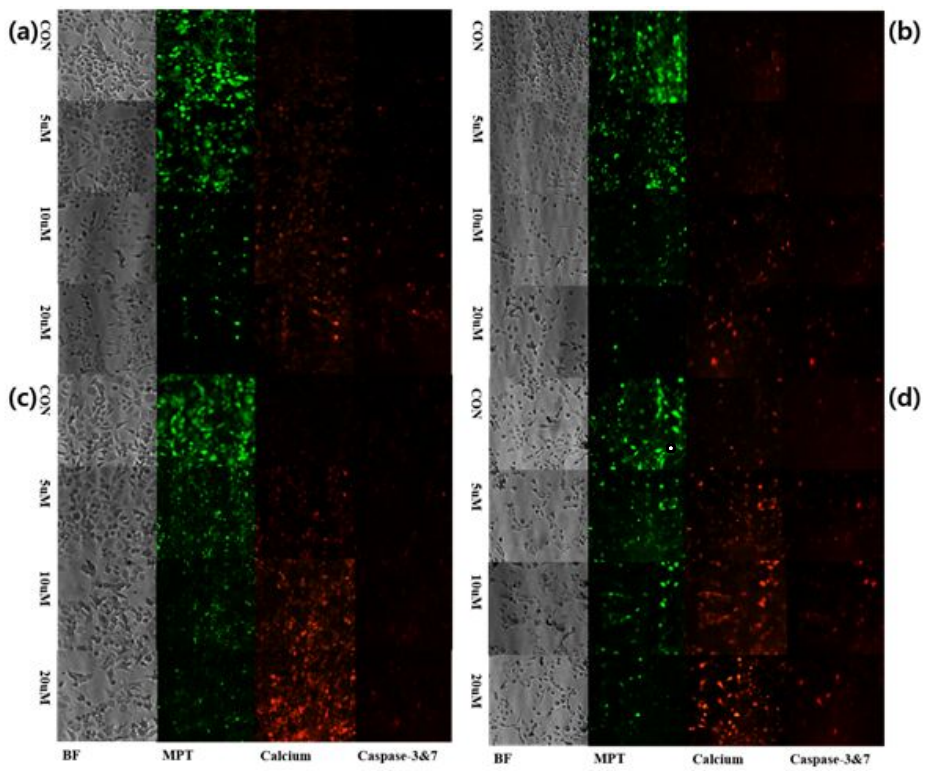

Figure 11A. High Content Screening Fluorescent Cellular Images The high content assay images obtained by utilizing an AOTF attached fluorescence microscope. (a) Treatment with DOPC-BTP. (b) Treatment with DOPE-BTP. (c) Treatment with M1-BTP. (d) Treatment with M2-BTP

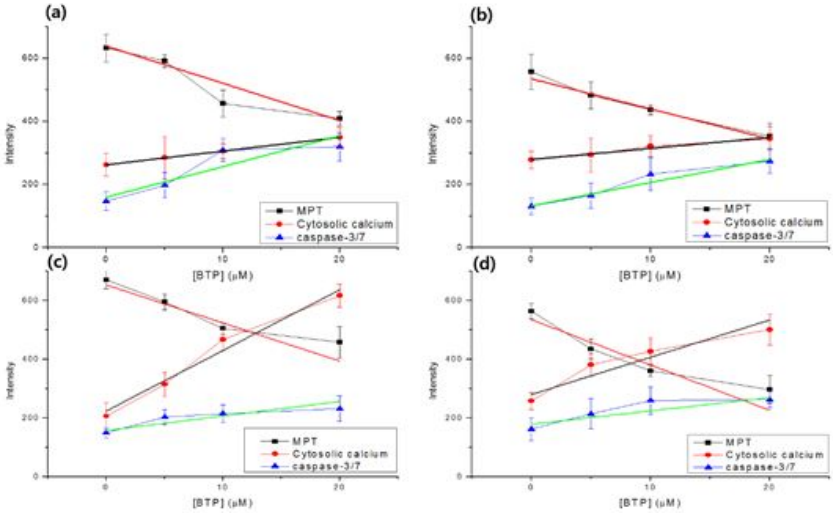

Figure 11B. High Content Screening Calculations

The graphical representation of the data present the average fluorescence of the cellular images. The error bars represent the standard deviation of the results. The assays were performed in triplicates. (a) Treatment with DOPC-BTP. (b) Treatment with DOPE-BTP. (c) Treatment with M1-BTP. (d) Treatment with M2-BTP

Figure 11A and 11B present the fluorescence images from the HCS assays and the graphical analysis of the results. The calcein fluorescence intensities of the PDT-treated cells decreased in a [BTP] dependent manner. The best fit line slopes of calcein fluorescence plot were calculated to be -11.79, -9.55, -12.98, and -15.45 for DOPC-BTP, DOPE-BTP, M1-BTP, and M2-BTP, respectively. M1-BTP and M2-BTP

treated cells exhibited greater decreases in the calcein fluorescence intensity, which is directly related to the magnitude of MPT. MCF-7 cells treated with liposomal-BTP and irradiation demonstrated elevations in their cytosolic calcium concentration. The best fit line slopes of calcium orange fluorescence intensity plots were calculated to be 4.35, 3.49, 20.65, and 12.68 for DOPC-BTP, DOPE-BTP, M1-BTP, and M2-BTP, respectively. Increases in the cytosolic calcium concentrations of the MCF-7 cells treated with PDT via ER-localizing M1-BTP and M2-BTP were much more significant compared to those of the MCF-7 cells treated with PDT via nucleus-localizing DOPC-BTP and DOPE-BTP. Even compared to the M2-BTP group, the M1-BTP treated cells exhibited a much greater calcium release. The concentration-dependent increase in the caspase-3/7 levels of the DNA localizing liposomal-BTP treated MCF-7 cells were greater than those of the ER localizing liposomal-BTP treated MCF-7 cells, confirmed by comparing their plot slopes (DOPC-BTP: 9.75, DOPE-BTP: 7.37, M1-BTP: 4.94, M2-BTP: 4.52).

Ⅳ. Discussion

The methods of synthesizing the novel photosensitizer, BTP, were easily reproducible. Results from the GC/MS FAB confirmed the m/z and purity of the compound. Among the different absorptive bands shown in the UV-Vis absorption spectrum, the local maxima at 600 nm was chosen for the irradiation wavelength. 600 nm was selected as the irradiation wavelength because of near-infrared radiation's ability to better penetrate human tissue. It has been reported that radiation scatters from inhomogeneous tissue structures at wavelengths below 600 nm, which may lead to an increase in undesired optical absorption[18]. The particle size distribution of the liposomes confirmed the successful formation of the small unilamellar liposomes. When liposomes contained the photosensitizer, the average diameters exhibited a general increase. This increase in diameter of the liposomes could be an indication of the successful liposomal encapsulation of BTP. The decrease in the absolute value of the BTP-encapsulated liposomes' zeta potentials were most likely an effect of the decrease in homogeneity in the biphospholipid layer of the vesicles. By introducing the photosensitizer molecules into the hydrophobic layer of the liposomes, the stability of the liposomes may be affected by molecular steric effects. Of the various liposomal compositions tested, DOPC liposomes were

the most stable, which led to the hypothesis that they may be the most effective in delivering BTP, as higher zeta potential has been reported to be accompanied by higher cellular uptake[19].

Before testing the photocytotoxicity of the liposomal-BTP, the cytotoxicity of the empty liposomes were tested (data not shown) in order to ensure that the liposomes were not damaging the MCF-7 cells. The various empty liposomes did not cause any significant decrease in the mitochondrial activity of the breast cancer cells even with radiation treatment of the 600 nm laser at 50 mW for 30 minutes. The anticancer activity of the DOPC-BTP was the most effective among the liposomal-BTPs tested. The rest of the liposomal-BTPs were less effective in reducing the mitochondrial activity of the MCF-7 cells. High colloidal stability of DOPC-BTP may be responsible for its efficient antitumor activity, confirming the correlation between colloidal stability and drug delivery efficiency.

The anticancer activity of photodynamic therapy is derived from the intracellular formation of the various ROS, resulting in the imbalance between the formation and elimination of ROS. 2',7'-dichlorofluorescein diacetate (DCFDA) is deacetylated by cellular esterases to a non-fluorescent compound, which is then oxidized by ROS into the highly fluorescent

2'7'-dichlorofluorescein (DCF). The MCF-7 cells treated with DOPC-BTP exhibited the highest concentration of intracellular ROS, which is in agreement with the corresponding photocytotoxicity. These results confirmed that 600 nm irradiation induced production of intracellular ROS by the BTP delivered by various liposomes. The concentration of intracellular ROS, the active component of the PDT-induced cancer cell death, was confirmed to be directly related to photocytotoxicity against MCF-7 cells.

PDT is known to have an effect only in the vicinity of the photosensitizing agent because most ROS are only able to travel about 0.03 μm[20]. Thus, the subcellular localization of BTP will directly correlate to the localization of the ROS. The nucleus localization of DOPC-BTP and DOPE-BTP were rather unexpected as its sulfonated derivative was reported to be mainly localized in the mitochondria and only partially in the nucleus. It can be inferred from the subcellular localization assays that the sulfonation of the photosensitizing molecule may be responsible for its affinity to the mitochondrial membrane. By sulfonating BTP at all four positions, its hydrophobicity decreases significantly as the sulfonic acid groups dramatically increase the molecule's polarity. Rangasamy et al. reported that the partial nucleus localization of the sBTP was feasible due to the π-π interaction between the aromatic structures of the DNA and the inner core of the porphyrin[5].

In order for the porphyrins to interact with DNA, the π-π interaction must be able to overcome the electrostatic repulsion. Compared to sBTP, BTP lacks the sulfonic acid moieties in its structure, which decreases the electrostatic repulsion of BTP against the negatively charged nucleus membrane.

Subcellular localizations of M1-BTP and M2-BTP were found to be in both the nucleus and the ER: a combination of the distinct localizing properties of the photosensitizer and the ER liposome, driven by its compositional similarity to the ER membrane. The ER liposomes have been reported to utilize a caveolin- and microtubule-dependent retrograde trafficking pathway to the ER membrane. The final destination of the liposomes, being endocytosed by either clathrin- or caveolae-dependent mechanisms, is dictated by both the cellular uptake route and the properties of the liposome itself[21]. A larger amount of BTP delivered via M2 liposomes was localized in the nucleus. Thus, it can be inferred that more of the M1-BTP is localized in the ER. The major factor in determining the localization of the different liposomes seems to be lipid composition. Pollock et al. patented a drug delivery system, comprised of different compositions of DOPC, DOPE, PS, and PI, that was able to localize in the ER in order to treat HIV viral infections[22]. It was observed that localization of the molecules delivered by liposomes could be controlled by

altering the lipid composition of the liposomes. As revealed in the intracellular localization assays of DOPC-TPPS and DOPE-TPPS in figure 11, DOPC and DOPE liposomes do not seem to have an effect in the localization properties of the delivery system. However, M1 and M2 liposomes, which contain four different lipids including DOPC and DOPE, caused ER localization of BTP along with partial localization in the nucleus. The ER localization of BTP was more distinct in M1-BTP. M1 and M2 lipid compositions contained the same ratio of PS and PI. These results signify the effect of the liposome composition on its subcellular localization. Localization of the photosensitizer in the ER represents the possibility of damaging the cell in an efficient manner since the ER is one of the largest calcium storages among the cellular organelles[23-25]. The disruption of its membrane leads to the increase in the cytosolic calcium concentration, disrupting the cytosolic calcium homeostasis of cells. One of the consequences of intracellular calcium homeostasis disruption is mitochondrial damage, which significantly contributes to cell death by resulting in the release of cytochrome c, damage of Bcl-2 anti-apoptotic protein member, activation of Bcl-2 pro-apoptotic protein, and activation of caspase cascades. The subcellular localization assays demonstrated the area of PDT action of the novel photosensitizer, BTP, delivered by various liposomes.

It has been established that fragmentation of DNA into high molecular weight molecules during the early stages of apoptosis can be monitored via gel electrophoresis[26]. The DNA fragmentation assay has since been widely used in detecting DNA damage[27]. High concentrations of retained photosensitizer in the nucleus may be responsible for the notable DNA damage in DOPC-BTP and DOPE-BTP treated MCF-7 cells. DNA fragmentation can be a direct result from the production of ROS in the vicinity of the nucleus; chromatin condensation, nuclear shrinkage, and cleavage of the DNase CAD (caspase activated deoxyribonuclease) inhibitor taking place after the cleavage of nuclear lamins[28]. Previously, studies on sBTP have confirmed the colocalization of sBTP in mitochondria and nucleus. sBTP PDT-induced genomic DNA fragmentation and caspase-mediated DNA damage has also been reported[5]. Figure 10 demonstrates that DOPC-BTP PDT and DOPE-BTP PDT are more effective than M1-BTP PDT and M2-BTP PDT in terms of causing apoptosis in cells by damaging the nucleus.

Three cellular markers were used to study the effects of the photodynamic photosensitizer's subcellular localization on the cell death pathways utilizing HCS: calcein-AM, calcium indicator orange, and caspase-3/7 substrate. Mitochondrial permeability transition (MPT) is defined as an increase in the permeability of the mitochondrial membrane to molecules less than 1500

daltons[29]. MPT pore (MPTP), an important factor in cell death, is a complex of the voltage-dependent anion channel, the adenine nucleotide translocase, and cyclophilin-D[30]. Acetoxymethyl esters of calcein dye are cleaved by the intracellular esterases to release the fluorescent calcein[31]. Mitochondrial calcein, which is unable to cross mitochondrial or plasma membrane, is known to rapidly exit the cell in the presence of MPTPs. Thus, the intracellular calcein fluorescence intensity in the HCS assays represents the magnitude of MPTP formation. The calcein fluorescence levels of the liposomal-BTP PDT-treated MCF-7 cells decreased in a concentration dependent manner, affirming the formation of MPTPs. Increase in cytosolic calcium, oxidative stress, and lipid breakdown products have been reported to result in MPT followed by the loss of proton gradient. Intracellular calcium homeostasis is a vital process in cell metabolism. An increase in the cytosolic calcium concentration to lethal levels is known to cause cellular damage and initiate cell death by phospholipid bilayer membrane disruption via phospholipase activation, disruption of membrane and cytoskeletal proteins via protease activation, cellular ATP depletion via ATPase activation, paralysis of energy-dependent Ca2+ pumps, and irreversible mitochondrial function inhibition[32,33]. Unlike the MCF-7 cells treated with a DNA-localizing liposomal photosensitizer (DOPC-BTP and DOPE-BTP), the MCF-7 cells treated with an

ER-localizing liposomal photosensitizer (M1-BTP and M2-BTP) exhibited remarkably larger elevations in cytosolic calcium concentrations. By cross-referencing the subcellular localization assay results with the HCS assay results, it can be inferred that the ER-localized BTP was able to produce sufficient oxidative stress in the ER membrane to cause the release of the stored calcium. Up-regulation and initiation of the caspase enzyme cascade is the central driving force in apoptotic cell death[34]. The caspase activity of the PDT-treated MCF-7 cells were monitored by utilizing a Magic Red™ (MR) caspase 3/7 assay kit. Although each liposomal-BTP was able to induce caspase-3/7 activity by photodynamic therapy in a concentration-dependent manner, MCF-7 cells treated with nucleus localizing liposomal-BTP exhibited greater levels of caspase-3/7 activity. DOPC-BTP exhibited the highest level of caspase-3/7 activity, corresponding with the rest of the data in this study. DOPC-BTP exhibited the smallest average diameter, highest colloidal stability, photocytotoxicity, and caspase-3/7 activity.

Although the ER-localizing liposomes, M1 and M2, were able to deliver BTP to both the nucleus and the ER, its antitumoral PDT activity was weaker than that of the DOPC-BTP, which was the liposomal-BTP with the highest colloidal stability. The ER-localizing liposomes also failed to induce DNA fragmentation, which may be a result of low BTP

concentrations localized at the nucleus. Since M1-BTP and M2-BTP target both the ER and the nucleus, their concentrations in each organelle may be much lower than that of the single organelle-targeting liposomal photosensitizers. If the ER-localizing liposomal-BTPs were able to produce both ER membrane damage and DNA fragmentation at significant levels, the PDT-induced anticancer activity of the ER-localizing liposomal-BTPs may be amplified significantly. Increasing the stability of the ER-localizing liposomes while maintaining its liposomal composition may be the next challenge in overcoming their current limitations.

Ⅴ. Conclusion

The successful application of various liposomes in delivering the hydrophobic photosensitizer, 5,10,15,20-tetrakis(benzo[b]thiophene), was confirmed. Liposomal BTPs exhibited significant photodynamic activity against MCF-7 breast cancer cells. DOPC-BTP and DOPE-BTP exhibited localization in the nucleus of the cells, while M1-BTP and M2-BTP were observed to be dually localized in the nucleus and ER. The subcellular destination of the photosensitizer seems to be manipulable by varying the lipid composition of the liposomes used to deliver the hydrophobic molecules. The application of ER liposomes, a targeting system based on compositional similarity with the ER membrane, enabled the delivery of BTP to the ER and nucleus of the breast cancer cells. Significant DNA damage was observed with irradiation in both nucleus localizing liposomal-BTPs. All liposomal BTP groups were able to induce MPTP formation and caspase-3/7 activation as observed from the HCS assays. Increase in the cytosolic calcium concentration was observed in the ER localizing M1-BTP and M2-BTP PDT treated MCF-7 cells.

Ⅵ. Reference

[1] Ahmad N, Feyes DK, Agarwal R, Mukhtar H. Photodynamic therapy results in induction of WAF1/CIP1/P21 leading to cell cycle arrest and apoptosis. Proceedings of the National Academy of Sciences. 1998;95(12):6977-82.

[2] Apel K, Hirt H. REACTIVE OXYGEN SPECIES: Metabolism, Oxidative Stress, and Signal Transduction. Annual Review of Plant Biology. 2004;55(1):373-99.

[3] Mroz P, Yaroslavsky A, Kharkwal GB, Hamblin MR. Cell death pathways in photodynamic therapy of cancer. Cancers. 2011;3(2):2516-39.

[4] Bhattacharjee S. The language of reactive oxygen species signaling in plants. Journal of Botany. 2012;2012.

[5] Rangasamy S, Ju H, Um S, Oh D-C, Song JM. Mitochondria and DNA Targeting of 5,10,15,20-Tetrakis(7-sulfonatobenzo[b]thiophene) Porphyrin-Induced Photodynamic Therapy via Intrinsic and Extrinsic Apoptotic Cell Death. Journal of Medicinal Chemistry. 2015;58(17):6864-74.

[6] Litzinger DC, Huang L. Biodistribution and immunotargetability of ganglioside-stabilized dioleoylphosphatidylethanolamine liposomes. Biochimica et Biophysica Acta (BBA)-Biomembranes. 1992;1104(1):179-87.

[7] Park S-H, Oh S-G, Mun J-Y, Han S-S. Loading of gold nanoparticles inside the DPPC bilayers of liposome and their effects on membrane fluidities. Colloids and Surfaces B: Biointerfaces. 2006;48(2):112-8.

[8] Pollock S, Antrobus R, Newton L, Kampa B, Rossa J, Latham S, et al. Uptake and trafficking of liposomes to the endoplasmic reticulum. FASEB journal : official publication of the Federation of American Societies for Experimental Biology. 2010;24(6):1866-78.

[9] Lindsey JS. The Synthesis of meso-Substituted Porphyrins. Metalloporphyrins Catalyzed Oxidations: Springer; 1994. p. 49-86.

[10] Kirby C, Clarke J, Gregoriadis G. Effect of the cholesterol content of small unilamellar liposomes on their stability in vivo and in vitro. The Biochemical journal. 1980;186(2):591-8.

[11] Simons K, Vaz WL. Model systems, lipid rafts, and cell membranes. Annual review of biophysics and biomolecular structure. 2004;33:269-95.

[12] Briuglia ML, Rotella C, McFarlane A, Lamprou DA. Influence of cholesterol on liposome stability and on in vitro drug release. Drug delivery and translational research. 2015;5(3):231-42.

[13] Michaelson D, Silletti J, Murphy G, D'Eustachio P, Rush M, Philips MR. Differential localization of Rho GTPases in live cells: regulation by hypervariable regions and RhoGDI binding. The Journal of cell biology. 2001;152(1):111-26.

[14] Lyklema J, Fleer GJ. Electrical contributions to the effect of macromolecules on colloid stability. Colloids and Surfaces. 1987;25(2):357-68.

[15] Hunter RJ, Midmore BR, Zhang H. Zeta Potential of Highly Charged Thin Double-Layer Systems. Journal of Colloid and Interface Science. 2001;237(1):147-9.

[16] Wang X, Roper MG. Measurement of DCF fluorescence as a measure of reactive oxygen species in murine islets of Langerhans. Analytical methods : advancing methods and applications.

2014;6(9):3019-24.
[17] Strauss WS, Gschwend MH, Sailer R, Schneckenburger H, Steiner R, Ruck A. Intracellular fluorescence behaviour of meso-tetra(4-sulphonatophenyl)porphyrin during photodynamic treatment at various growth phases of cultured cells. Journal of photochemistry and photobiology B, Biology. 1995;28(2):155-61.
[18] Schmidt-Erfurth U, Hasan T. Mechanisms of Action of Photodynamic Therapy with Verteporfin for the Treatment of Age-Related Macular Degeneration. Survey of Ophthalmology. 2000;45(3):195-214.
[19] Honary S, Zahir F. Effect of zeta potential on the properties of nano-drug delivery systems-a review (Part 1). Tropical Journal of Pharmaceutical Research. 2013;12(2):255-64.
[20] Salet C, Moreno G, Ricchelli F, Bernardi P. Singlet oxygen produced by photodynamic action causes inactivation of the mitochondrial permeability transition pore. Journal of Biological Chemistry. 1997;272(35):21938-43.
[21] Sonnichsen B, De Renzis S, Nielsen E, Rietdorf J, Zerial M. Distinct membrane domains on endosomes in the recycling pathway visualized by multicolor imaging of Rab4, Rab5, and Rab11. The Journal of cell biology. 2000;149(4):901-14.
[22] Pollock S, Dwek RA, Zitzmann N. Endoplasmic reticulum targeting liposomes. Google Patents; 2009.
[23] Meldolesi J, Pozzan T. The endoplasmic reticulum Ca 2+ store: a view from the lumen. Trends in biochemical sciences. 1998;23(1):10-4.
[24] Koch GL. The endoplasmic reticulum and calcium storage. Bioessays. 1990;12(11):527-31.

[25] Lytton J, Westlin M, Burk SE, Shull GE, MacLennan DH. Functional comparisons between isoforms of the sarcoplasmic or endoplasmic reticulum family of calcium pumps. Journal of Biological Chemistry. 1992;267(20):14483-9.

[26] Schwartz DC, Cantor CR. Separation of yeast chromosome-sized DNAs by pulsed field gradient gel electrophoresis. Cell. 1984;37(1):67-75.

[27] Gavrieli Y, Sherman Y, Ben-Sasson SA. Identification of programmed cell death in situ via specific labeling of nuclear DNA fragmentation. The Journal of cell biology. 1992;119(3):493-501.

[28] Savill J, Fadok V. Corpse clearance defines the meaning of cell death. Nature. 2000;407(6805):784-8.

[29] Lemasters JJ, Theruvath TP, Zhong Z, Nieminen A-L. Mitochondrial Calcium and the Permeability Transition in Cell Death. Biochimica et biophysica acta. 2009;1787(11):1395-401.

[30] Crompton M. The mitochondrial permeability transition pore and its role in cell death. The Biochemical journal. 1999;341 (Pt 2):233-49.

[31] Petronilli V, Miotto G, Canton M, Brini M, Colonna R, Bernardi P, et al. Transient and Long-Lasting Openings of the Mitochondrial Permeability Transition Pore Can Be Monitored Directly in Intact Cells by Changes in Mitochondrial Calcein Fluorescence. Biophysical Journal. 1999;76(2):725-34.

[32] Criddle D, Gerasimenko JV, Baumgartner H, Jaffar M, Voronina S, Sutton R, et al. Calcium signalling and pancreatic cell death: apoptosis or necrosis? Cell Death & Differentiation. 2007;14(7):1285-94.

[33] Nomura M, Ueno A, Saga K, Fukuzawa M, Kaneda Y.

Accumulation of cytosolic calcium induces necroptotic cell death in human neuroblastoma. Cancer research. 2014;74(4):1056-66.
[34] Earnshaw WC, Martins LM, Kaufmann SH. Mammalian caspases: structure, activation, substrates, and functions during apoptosis. Annual review of biochemistry. 1999;68(1):383-424.

국문 초록

현대 과학의 발달로 인해서 항암치료기술이 상당한 속도로 빠르게 발전하고 있다. 하지만 항암치료의 가장 큰 장애물은 항암물질들이 건강한 세포들에 미치는 영향이다. 암세포를 죽이는 역할을 하는 물질들이 비특이적으로 인체의 세포들에게도 독성을 지니기 때문이다. 그 비특이성 세포 독성이 항암치료 환자들의 부작용에 대한 주원인이다. 항암치료에 대한 부작용을 감소시키기 위한 전략은 암세포를 특정하게 대상하는 항암치료 시스템이다. 그 중에 광역학요법은 암세포에 국소화되는 감광제나 특정 부위에 방사능을 처리함으로써 건강한 세포들에게 미치는 세포 독성을 최소화하는 기술이다. 이 연구에서는 리포좀으로써 전달되는 포르피린을 이용한 target-specific 광역학요법 시스템을 이용하였다.

5,10,15,20-tetrakis(benzo[b]thiophene) porphyrin (BTP)는 새로 합성한 소수성 포르피린이다. 이전에는 BTP의 제한된 용해성으로 인해, 물질에 대한 광역학적 연구가 불가능하였다. 따라서 이를 해결하기 위해 다양한 지질구성을 가진 리포좀을 이용해서 BTP의 용해도를 바꿀 수 있었다. 이 연구에서는 리포좀-BTP에 대한 광세포독성, 활성산소발생역량, 세포내 localization을 확인하였다. DNA 분열 분석과 High Content Screening (HCS) 실험들은 리포좀-BTP의 항암활성도의 메커니즘을 연구하기 위해 진행하였다. MTT assay를 통해 리포좀-BTP의 특정 대상 항암활성도를 확인하고 리포좀-BTP의 농도에 따른 활성산소발생력 또한 증명하였다. Localization 실험을 통해 여러 가지 리포좀-BTP에 의한 BTP localization은 감광제만의 성질뿐만 아니라 전달 에이전트인 리포좀의 성질에 의해서 결정된다는 것을 확인하였다. 이를 통하여 리포좀들의 세포 localization을 결정하는 본질적인 요인은 리포좀들의 지질구성으로 추정된다. 광역학요법을 통해 DNA-localizing 리포좀-BTP들은 상당한 양의 DNA 분열을 일으켰고 모든 리포좀-BTP들은 유방암 세포들의 미토콘드리아 투수성이행, 시토졸 칼슘 농도, 카스파제-3/7 활성화에 주목할 만한 영향을 주는 것을 확인하였다.

주요어

광역학요법, 리포좀, High Content Screening, Localization

학번: 2014-21971